



HAL
open science

EFFECTIVENESS OF AVALANCHE PROTECTION STRUCTURES IN RUN-OUT ZONES: THE TACONNAZ AVALANCHE PAST CASE IN FRANCE

Mohamed Naaim, Thierry Faug, F. Naaim-Bouvet, Nicolas Eckert

► **To cite this version:**

Mohamed Naaim, Thierry Faug, F. Naaim-Bouvet, Nicolas Eckert. EFFECTIVENESS OF AVALANCHE PROTECTION STRUCTURES IN RUN-OUT ZONES: THE TACONNAZ AVALANCHE PAST CASE IN FRANCE. International Snow Science Workshop, Oct 2018, Innsbruck, Austria. hal-01997841

HAL Id: hal-01997841

<https://hal.science/hal-01997841>

Submitted on 13 Feb 2019

HAL is a multi-disciplinary open access archive for the deposit and dissemination of scientific research documents, whether they are published or not. The documents may come from teaching and research institutions in France or abroad, or from public or private research centers.

L'archive ouverte pluridisciplinaire **HAL**, est destinée au dépôt et à la diffusion de documents scientifiques de niveau recherche, publiés ou non, émanant des établissements d'enseignement et de recherche français ou étrangers, des laboratoires publics ou privés.

EFFECTIVENESS OF AVALANCHE PROTECTION STRUCTURES IN RUN-OUT ZONES: THE TACONNAZ AVALANCHE PAST CASE IN FRANCE

Mohamed Naaim¹, Thierry Faug^{1,*}, Florence Naaim-Bouvet¹, Nicolas Eckert¹

¹Univ. Grenoble Alpes, Irstea, UR ETGR, France

ABSTRACT: The present study uses a numerical avalanche propagation model based on depth-averaged equations supplemented with the Voellmy snow rheology. The effectiveness of the complex avalanche protection system currently built in the run-out zone of Taconnaz avalanche path, in the French Alps in Chamonix Mont-Blanc valley, is evaluated. This work was motivated by the fact that the protection structure initially planned to mitigate a centennial reference avalanche event could not be fully achieved primarily due to some budgetary constraints. A number of numerical simulations were conducted, considering different avalanche scenarios in terms of both the volume and the Froude number of the incoming flows at the entrance of the current avalanche protection system. Particular attention was paid to the residual volumes that were able to overtop the 25-m-high catching dam settled at the downstream end of the avalanche protection system, thus quantifying the overall effectiveness of the current protection system for the different scenarios considered.

Keywords: Avalanche, retarding mounds and dams, depth-averaged model, protection effectiveness.

1. INTRODUCTION

Protection structures, such as retarding mounds, deflecting and catching dams, can be built in avalanche run-out zones in order to dissipate avalanche energy, deflect and finally stop dense flows. The design of avalanche protection dams received much attention over the last two decades. A number of research projects allowed to develop new European guidelines (Barbolini et al. , 2009) which are mainly based on the application of shallow-water shock theory to travelling shocks formed in snow avalanches, assimilated to rapid granular flows, when they meet obstacles (Gray et al. , 2003; Hákonardóttir and Hogg , 2005; Faug et al. , 2007). Note that recent studies highlighted the need of still improving the description of granular flows around obstacles (Faug , 2015) and of the formation of such granular shocks in particular (Faug et al. , 2015; Méjean et al. , 2017), in order to improve avalanche propagation models in the future.

The present paper gives an example on how available avalanche propagation models based on depth-averaged equations can be used to evaluate the effectiveness of protection structures. The case study considered is the large protection system built in the run-out zone of Taconnaz avalanche path in Chamonix Mont-Blanc valley (in the French Alps). Irstea was asked by the local municipalities to evaluate the effectiveness of the currently built protec-

tion system with the help of numerical modelling. Section 2 presents briefly the context of the study. Section 3 gives a short description of the avalanche propagation model used based on depth-averaged equations. Section 4 addresses the numerical results concerning the effectiveness of the currently built avalanche protection system at Taconnaz, considering different avalanche scenarios in terms of volume and Froude number of the incoming flow. Finally, the main results are summarized and challenging questions are discussed in Section 5.

2. BUILT VERSUS PROJECTED TACONNAZ PROTECTION SYSTEM

Figure 1 shows the protection system projected at Taconnaz avalanche path, as well as the currently built system which was achieved in 2012. The projected protection system was designed by Irstea combining a wide spectrum of approaches: morphological study of the site, historical data analysis, back-calculation of past recorded events on the avalanche path using a numerical avalanche propagation model (this model will be shortly described in Sec. 3), statistical analysis of the numerical results for the definition of the 100–years return period scenarios, physical and numerical modelling of the dense flow-obstacle interaction in the runout zone for the optimization of the protection system, and analysis of the residual risk associated with potential powder avalanches using physical and numerical models. A summary of that work can be found in Naaim et al. (2010).

By cross-comparing the top and bottom panels shown in Figure 1, one can identify the main dif-

*Corresponding author address:

Thierry Faug, Univ. Grenoble Alpes, Irstea, UR ETGR,
2 rue de la Papeterie BP 76, F-38402 Saint Martin d'Heres;
tel: +33 4 28 28 76 76; fax: +33 4 76 51 38 03
email: thierry.faug@irstea.fr

ferences between the project (top panel) and the built-up protection system (bottom panel). Among the six retarding mounds projected, two mounds (T4 and T6 on Figure 1) were not achieved. A remaining piece of the former lateral confining dam (built in 1990), although the resistance of that piece to avalanche impact is very uncertain, may currently play the role of mound T6. A part of a former deflecting spike may contribute to fulfill some of the functions of the initially projected mound T4. Also, the intermediate 7.5-m-high dam designed for appropriate repartition (storage and dissipation) of the snow mass into the areas downstream of the retarding mounds and upstream of the frontal 25-m-high dam was not built-up. Rock and soil materials extracted during the construction of the new protection structures still remain in the deposition area upstream of the frontal 25-m-high dam. Finally, the whisker dams downstream of the frontal dam and designed to contain the snow mass able to go through the torrent control hydraulic structure are absent.

Existence of some significant differences between the project and the system achieved in 2012 makes the currently built protection system less efficient than initially designed. In particular, it is straightforward that the volume ($\sim 1.6 \text{ Mm}^3$) of the 100-years return period (single) avalanche event (other 100-years return period events were studied, considering two successive 10-years return period avalanches), travelling with a Froude number of 4.3 (Naaïm et al. (2010)), can not be fully stopped by the current protection system. The Froude number is defined here as $Fr = \bar{u} / \sqrt{gh}$, where h is the flow thickness, \bar{u} is the depth-averaged velocity and g the gravity acceleration ($g = 9.81 \text{ m.s}^{-2}$).

The overarching aim of the present paper is to summarize the results in terms of the effectiveness of the currently built protection system (Sec. 4) obtained from numerical simulations for a range of avalanche scenarios from the (single) centennial event mentioned above to other avalanche scenarios of lower magnitude in terms of volumes and Froude number of the flow at the entrance of the protection system. In the following section, we briefly describe the avalanche model used and the main assumptions made.

3. THE AVALANCHE PROPAGATION MODEL

3.1. Brief model description

The avalanche propagation model used in the current study is based on the depth-averaged mass and momentum conservation equations:

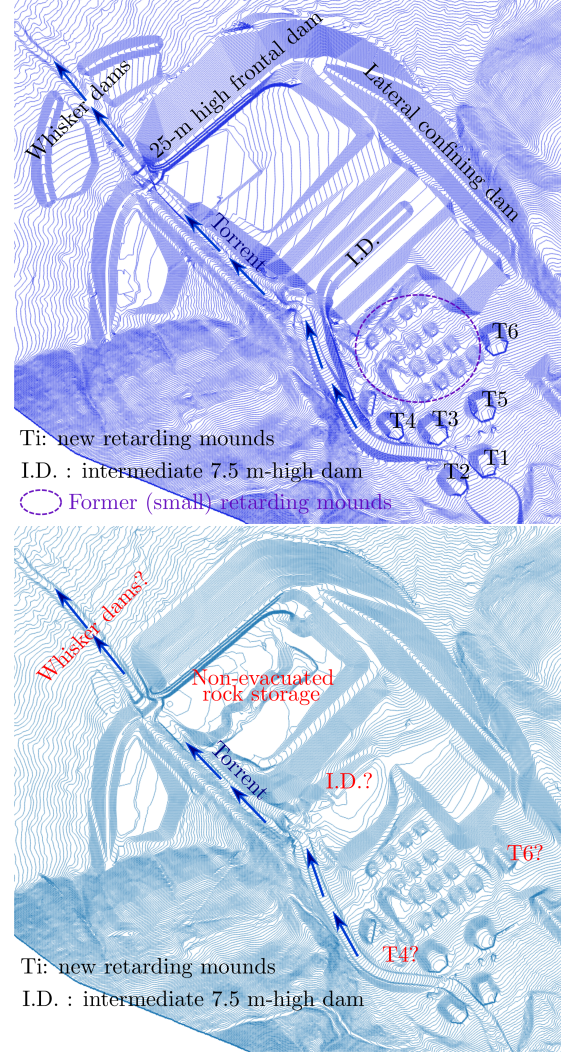


Figure 1: Digital terrain models of the projected protection system (top) and the currently built protection system whose construction was achieved at the end of year 2012 (bottom).

$$\frac{\partial h}{\partial t} + \frac{\partial h\bar{u}}{\partial x} = \Phi_{e/d}, \quad (1)$$

$$\frac{\partial h\bar{u}}{\partial t} + \beta \frac{\partial h\bar{u}^2}{\partial x} = gh \cos \theta \left(\tan \theta - \mu - k \frac{\partial h}{\partial x} \right), \quad (2)$$

supplemented with the Voellmy constitutive law usually used for the flowing snow:

$$\mu = \mu_0 + \frac{g}{\xi} Fr^2, \quad (3)$$

where μ is the effective friction, and μ_0 and ξ hold for the two frictional parameters. The coefficient β depends on the shape of the velocity profile and is defined by $\bar{u}^2 = \beta \bar{u}^2$, and k is the earth pressure coefficient which can account for non-isotropic hydrostatic pressure distribution.

The above equations in their one-dimensional (1D) form correspond to a reduced form of the

two-dimensional (2D) mass (Eq.(1)) and momentum (Eq.(2)) conservation equations actually implemented in the numerical model. Details can be found in Naaim et al. (2004). It is worthy to note that the equation system, written under its conservative form (Naaim, 1998), is solved with a Godunov finite volumes scheme (Godunov, 1959). The equations are integrated over each cell. The use of unstructured mesh makes the introduction of complex geometries easy. The mesh can be adapted to the presence of obstacles or slope variations. The exact expression used for the erosion/deposition flux $\Phi_{e/d} = dz/dt$ is described in detail in Naaim et al. (2004). Note that the erosion/deposition model was carefully checked against some specific laboratory tests on granular deposits forming against a rigid barrier down an incline (Faug et al., 2004). The topographic surface of the bottom is recalculated after each time step so as to take into account the erosion and deposition fluxes. All those features, including the use of unstructured mesh, the shocks capturing scheme, the modelling of curvature effects, the erosion/deposition model and the recalculation of the exact topography of the topographic surface—although those features can all be still improved, make the numerical code used in the present study very efficient at simulating in a proper manner the complicated interaction between the avalanche-flow and the complex protection system of Taconnaz (see Figure 2).

3.2. Simulation example for Taconnaz

A wide spectrum of avalanche scenarios at the entrance of the protection system was considered in the present study. Total volumes were varied from about $800\,000\text{ m}^3$ to about 1.8 Mm^3 , for three values of the Froude number of the flow at the entrance of the protection system: $Fr = 2.9$ (typical of the snow conditions during winter 1999), $Fr = 4.3$ (value of the centennial single event, as described in (Naaim et al., 2010)) and an intermediate value $Fr = 3.8$. It is worthy to note that the numerical simulations were performed in the run-out zone only, by specifying the shape of the hydrograph (evolution of flow discharge over time) at the entrance of the protection system depending on both V and Fr . The shapes of the hydrographs were initially established thanks to a series of numerical simulations all along the avalanche path to back-calculate historical events based on observed volumes, departure zones and run-out distances (as available in the French EPA "Enquête Permanente sur les Avalanches" (Naaim et al., 2010)).

Figure 2 displays an example of avalanche simulation results for an intermediate avalanche scenario specifying the hydrograph at the entrance of the protection system with $V = 1\,256\,800\text{ m}^3$ and

$Fr = 3.8$. The retarding mounds are efficient to dissipate the energy of the incoming flow and spread the incoming mass. However, the relatively high Froude number, corresponding to a low snow friction, prevents final significant storage in the areas around the new (large) and former (small) retarding mounds. That the 7.5-m-high intermediate dam is absent also reduces the storage capacity in the upper part of the protection system. Most of the mass is stored behind the 25-m-high frontal dam but a significant mass is able to go through the torrent hydraulic structure and spread along the torrent downstream of the frontal dam. For that specific scenario, the overtopping volume (downstream of the frontal dam) was evaluated to be about $30\,000\text{ m}^3$.

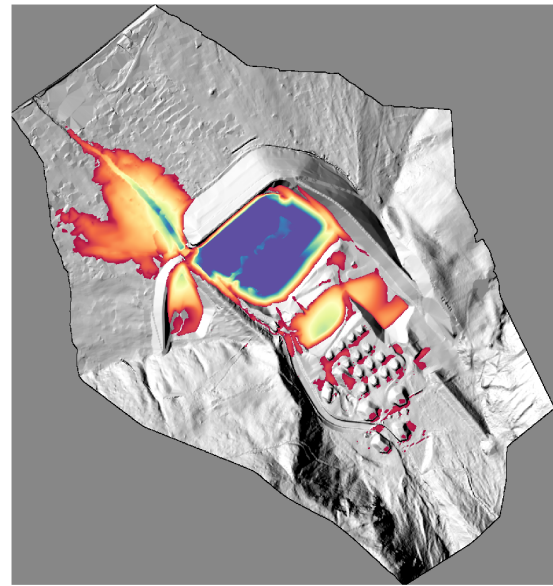


Figure 2: Simulation of an avalanche propagating in the currently built protection system (achieved in 2012): example of the final deposit for $V = 1\,256\,800\text{ m}^3$ and $Fr = 3.8$ as input conditions for the hydrogram at the entrance of the protection system.

4. EFFECTIVENESS OF THE CURRENT TACONNAZ PROTECTION SYSTEM

4.1. Volumes overtopping the dam

Figure 3 displays the volume able to overtop the 25-m-high catching dam, noted V_{over} , as a function of the total avalanche volume for the three values of the Froude number tested. The curves show that V_{over} increases with Fr . The increase is more pronounced at high Fr , as depicted in the inset of Figure 3. The plots show that rapid flows ($Fr = 4.3$ or 3.8) are able to overtop the dam regardless of the initial avalanche volume considered. In contrast, only the avalanche with large volumes, typically greater than 1.2 Mm^3 , can still overtop the dam, considering a lower $Fr = 2.9$ (which corresponds to the snow type involved during winter 1999). For

a very fluidized snow ($Fr = 4.3$), the overtopping volume increases from 20 000m³ for a total volume equal to 870 000m³ to 250 000m³ for a total volume slightly greater than 1.75Mm³.

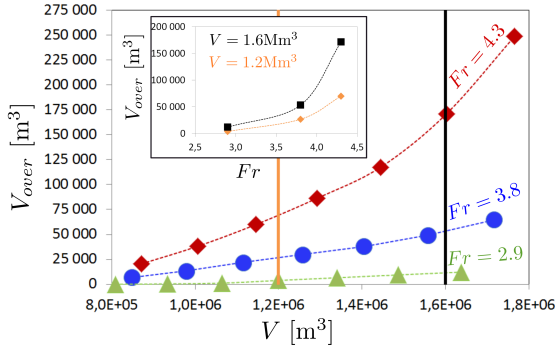


Figure 3: Overtopping volume, V_{over} , versus the total avalanche volume, V , for three values of the incoming Froude number, Fr . Inset: V_{over} versus Fr for two values of V .

4.2. Protection system efficiency

We now define the efficiency \mathcal{E} of the protection system as it follows:

$$\mathcal{E} = 100 \times \frac{V - V_{over}}{V}, \quad (4)$$

expressed as a percentage. Figure 4 shows the efficiency \mathcal{E} calculated by the avalanche propagation model presented in Sec. 3, considering different avalanche scenarios in terms of avalanche volume and Froude number of the incoming flow. It can be concluded that, for a given Fr , the efficiency of the protection system decreases with the increase of the total avalanche volume. The loss of efficiency is more pronounced for higher Fr , as shown in inset of Figure 4. For avalanches with a total volume smaller than 1.2Mm³ and characterized by $Fr = 2.9$ (typical of the event which occurred in winter 1999), the efficiency of the protection system currently build is 100%. For larger V and $Fr = 2.9$, the efficiency is below 100%. For $Fr = 3.8$ and $Fr = 4.3$, the efficiency is below 100% regardless of the total avalanche volume. For $Fr = 4.3$, this yields an efficiency that is slightly higher than 97.5% for a total volume of 870 000m³. Still for $Fr = 4.3$, the efficiency drops down to less than 86% for a total volume slightly greater than 1.75Mm³.

5. DISCUSSION AND CONCLUSION

The present study allowed to illustrate how a numerical avalanche propagation model could be used to analyze the effectiveness of a complex avalanche protection system made of a combination of dissipating, deflecting and catching structures. A set of

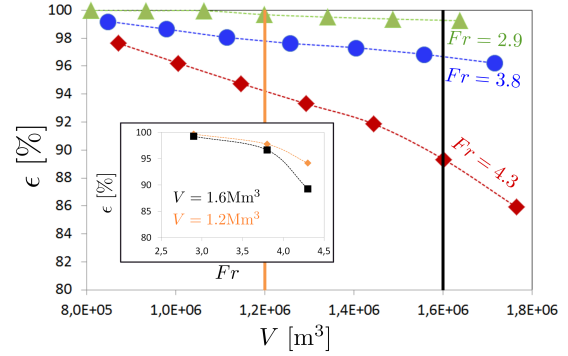


Figure 4: Efficiency \mathcal{E} of the Taconnaz protection system versus the total avalanche volume, V , for three values of the incoming Froude number Fr . Inset: \mathcal{E} versus Fr for two values of V .

avalanche scenarios, with different initial avalanche volumes (from 870 000m³ to 1.75Mm³) and incoming Froude numbers (from 2.9 to 4.3) as input conditions at the entrance of the protection system, was considered. Attention was then paid to volumes capable of overtopping the 25–m-high catching dam, highlighting the differences in terms of overtopping volumes between the currently built protection system and the initial project. Future research will consider other metrics of effectiveness evaluation, such as “inundation” areas downstream of the 25–m-high dam, velocities, and even individual risks considering a simple vulnerability function and calculating the integral over the inundation areas.

On another note, it is interesting to stress that the method used here shows the existence of a critical Froude number above which the overtopping volumes drastically increase (see inset of Figure 3), leading to a significant drop in efficiency of the protection system (see inset of Figure 4). Beyond the specific case study investigated here, this result reinforces the idea that it is crucial to consider the avalanche volume and how fast this volume travels down the slope as well, when designing protection structures against snow avalanches. The capacity of the avalanche to travel more or less fast was captured in the present study by varying the Froude number, which is considered as a good indicator of the effective friction of the snow, provided that the liquid water content remains below a certain value. However, it has been recently shown that above a certain amount of liquid water content, the effective friction can drastically decrease (Naaim et al. , 2013). The potential danger of those lubricated wet-snow avalanches able to travel large distances when they involve large volumes—although their Froude number are relatively small—will need further investigations in the future. Yet, a full description of the complex behaviour of a wet-snow avalanche and its interaction with protection structures remains today very challenging. In particular those slow wet-snow avalanches are known to exhibit puzzling tra-

jectories and produce complex deposits with patterns that resemble enormous octopus or squid tentacles. The wet-snow deposits are characterized by a rough and coarse-grain surface and levées that are salient signatures of granular segregation and fingering processes. This is in strong contrast with faster dry (or slightly wet) dense-flow avalanches that form more uniformly spread deposits. The latter are quite well-captured by current depth-averaged models, such as the one used in the present study. Efforts should be made in the future to develop new theories, and the underpinning avalanche propagation numerical models, capable of accounting for this intricate physics. The measurements made with GEODAR (see (Köhler et al. , 2018) and references therein) can help in quantifying some details of that intricate physics and testing the future models.

ACKNOWLEDGEMENT

The present study was undertaken under an expertise contract between Irstea and the local municipalities ("Communauté de Communes de la Vallée de Chamonix Mont-Blanc"). This work is supported by the French National Research Agency in the framework of the Investissements d'Avenir program (ANR-15-IDEX-02).

REFERENCES

- Barbolini, M., U. Domaas U., T. Faug, P. Gauer, K.M. Hákonardóttir, C.B. Harbitz, D. Issler, T. Jóhannesson, K. Lied, M. Naaim, F. Naaim-Bouvet, and L. Rammer (2009). The design of avalanche protection dams. Recent practical and theoretical developments. European Commission, Directorate-General for Research, Publication EUR 23339, 2009. Edited by T. Jóhannesson, P. Gauer, D. Issler and K. Lied.
- Faug, T., M. Naaim, and F. Naaim-Bouvet (2004). Experimental and numerical study of granular flow and fence interaction. *Annals of Glaciology*, 38, 135-138.
- Faug, T., M. Naaim, and A. Fourrière A. (2007). Dense snow flowing past a deflecting dam: an experimental investigation. *Cold Regions Science and Technology*, 49, 64-73.
- Faug, T. (2015). Depth-averaged analytic solutions for free-surface granular flows impacting rigid walls down inclines. *Physical Review E*, 92, 062310.
- Faug, T, P. Childs, E. Wyburn, and I. Einav I. (2015). Standing jumps in shallow granular flows down smooth inclines. *Physics of Fluids*, 27, 073304.
- Godunov, S. K. (1959). A difference method for numerical calculation of discontinuous solutions of the equations of hydrodynamics. *Mat. Sb. (N.S.)*, 47(89):3, 271-306.
- Gray, J.M.N.T., Y.-C. Tai, and S. Noelle (2003). Shock waves, dead-zones and particle-free regions in rapid granular free surface flows. *Journal of Fluid Mechanics*, 491, 161-181.
- Hákonardóttir, K. M. and A.J. Hogg (2005). Oblique shocks in rapid granular flows. *Physics of Fluids*, 17, 077101.
- Köhler, A., J.N. McElwaine, and B. Sovilla, B. (2018). GEODAR Data and the Flow Regimes of Snow Avalanches. *Journal of Geophysical Research: Earth Surface*, 123.
- Méjean, S., T. Faug, and I. Einav (2017). A general equation for standing normal jumps in both hydraulic and dry granular flows. *Journal of Fluid Mechanics*, 816, 331-351.
- Naaim, M. (1998). Dense avalanche numerical modeling, interaction between avalanche and structures. In: Hestnes, E. (Ed.), 25 years of avalanche research, Voss 12–16 May 1998, Proceedings, Oslo., 187-291 (NGI Publications 203).
- Naaim, M., F. Naaim-Bouvet, T. Faug, and A. Bouchet (2004). Dense snow avalanche modeling: flow, erosion, deposition and obstacle effects. *Cold Regions Science and Technology*, 39(2/3), 193-204.
- Naaim, M., T. Faug, F. Naaim-Bouvet, and N. Eckert (2010). Return period calculation and passive structure design at the Taconnaz avalanche path, France. *Annals of Glaciology*, 51(54), 89-97.
- Naaim, M., Y. Durand, N. Eckert, and G. Chambon (2013). Dense avalanche friction coefficients: Influence of physical properties of snow. *Journal of Glaciology*, 59(216), 771-782.